Toward the Sustainable Synthesis of Propanols from Renewable Glycerol over MoO$_3$-Al$_2$O$_3$ Supported Palladium Catalysts

Shanthi Priya Samudrala *[ID] and Sankar Bhattacharya[ID]

Department of Chemical Engineering, Faculty of Engineering, Monash University, Melbourne 3800, Australia; sankar.bhattacharya@monash.edu
*   Correspondence: priya.shanthipriya@monash.edu; Tel.: +61-3-9905-8162

Abstract: The catalytic conversion of glycerol to value-added propanols is a promising synthetic route that holds the potential to overcome the glycerol oversupply from the biodiesel industry. In this study, selective hydrogenolysis of 10 wt% aqueous bio-glycerol to 1-propanol and 2-propanol was performed in the vapor phase, fixed-bed reactor by using environmentally friendly bifunctional Pd/MoO$_3$-Al$_2$O$_3$ catalysts prepared by wetness impregnation method. The physicochemical properties of these catalysts were derived from various techniques such as X-ray diffraction, NH$_3$-temperature programmed desorption, scanning electron microscopy, ^{27}Al NMR spectroscopy, surface area analysis, and thermogravimetric analysis. The catalytic activity results depicted that a high catalytic activity (>80%) with very high selectivity (>90%) to 1-propanol and 2-propanol was obtained over all the catalysts evaluated in a continuously fed, fixed-bed reactor. However, among all others, 2 wt% Pd/MoO$_3$-Al$_2$O$_3$ catalyst was the most active and selective to propanols. The synergic interaction between the palladium and MoO$_3$ on Al$_2$O$_3$ support and high strength weak to moderate acid sites of the catalyst were solely responsible for the high catalytic activity. The maximum glycerol conversion of 88.4% with 91.3% selectivity to propanols was achieved at an optimum reaction condition of 210 °C and 1 bar pressure after 3 h of glycerol hydrogenolysis reaction.

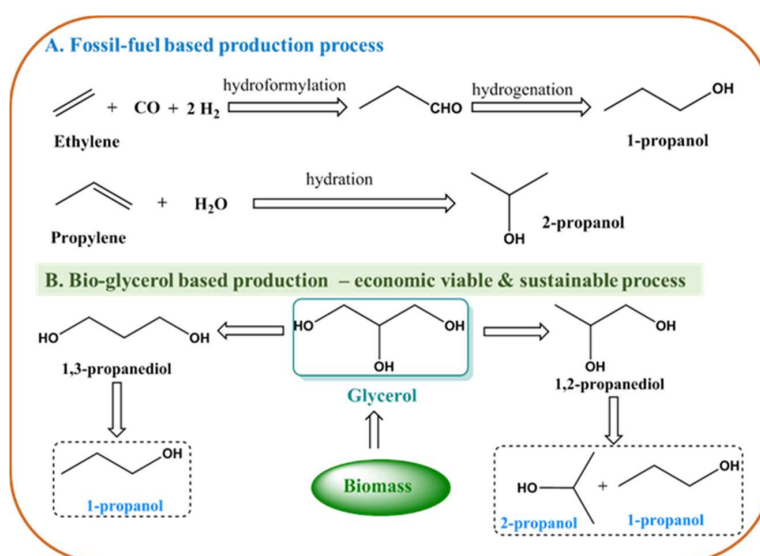**Keywords:** hydrogenolysis; glycerol; 1-propanol; 2-propanol; palladium catalyst

1. Introduction

Alternate sustainable energy resources are vital because of dwindling petroleum reserves and mounting environmental alarms that are allied with fossil fuel exploitation. As a result, alternative bio-based fuels have emerged as the long-standing solution as they are renewable and carbon dioxide neutral [1]. Biodiesel is one such alternative fuel which has received much attention with both demand and production tremendously increased over the last few years. However, along with biodiesel, also known as alkyl esters of long chain fatty acids (C14–C24), a great deal of glycerol as a by-product is also generated, typically equaling 10% of the whole production volume. The crude glycerol, if not handled properly, ends up as a waste product that has low value and is costly to purify in addition to jeopardizing the environmentally friendly nature of the whole biodiesel production process [2]. Valorization of glycerol is, therefore, necessary to enhance the sustainability of the biodiesel industry.

Glycerol, the simplest tri-hydroxy alcohol, is a highly versatile product, with many potential applications. The biodegradability and multi-functional nature of glycerol makes it a promising precursor for the production of high-value bio-renewable fuel/chemical products through various processes involving heterogeneous catalysis, e.g., acetalization [3,4], esterification [5], etherification [6], oxidation [7], dehydration [8], hydrogenolysis [9], and catalytic reforming [10]. The glycerol-derived

fuel and chemical products include liquid/gaseous fuels, fuel additives, and chemicals such as solketal, glycerol mono-esters, glyceric acid, 1,3-dihydroxyacetone, epichlorohydrin, glycidol, tartronic acid, lactic acid, acrylonitrile, 1,2-propanediol, and 1,3-propanediol, etc. Catalytic hydrogenolysis of glycerol is a promising approach, resulting in the formation of commodity chemicals such as 1,2-propanediol, 1,3-propanediol, ethylene glycol, propanols (1-propanol and 2-propanol), lower alcohols, and hydrocarbons [11]. Significant efforts have been made to convert glycerol into propanediols, but direct production of propanols via glycerol hydrogenolysis received limited attention.

1-propanol (1-PrOH) and 2-propanol (2-PrOH) are valuable commodity chemicals conventionally produced from fossil-based feedstocks ethylene and propylene by hydroformylation-hydrogenation and hydration reaction processes, respectively [12]. 1-PrOH has potential applications, primarily as a solvent in the pharmaceutical, paint, cosmetics, and cellulose ester industries, organic intermediate for the synthesis of important chemical commodities, and considered as the next-generation gasoline to petroleum substitute. 2-PrOH is extensively used as an industrial solvent and disinfectant, with major applications in the pharmaceutical industry and auto industry [13]. Due to the growing demand of these commodities, the production of 1-PrOH and 2-PrOH based on bio-based glycerol (Scheme 1) appears to be an attractive approach regarding sustainability and energy efficiency compared to the process based on petroleum-derived feedstocks.

Scheme 1. Synthetic routes to 1-propanol and 2-propanol.

Hydrogenolysis of glycerol generally takes place via the dehydration-hydrogenation pathway over metal-acid bifunctional catalysts [8,14–16]. Noble metal-based catalysts have proven to be highly effective for glycerol hydrogenolysis [17]. Very few catalytic systems based on Ni [18], Ir [19], Rh [20,21], Pt [22,23], and Ru [24,25] based catalysts have so far been reported for the direct synthesis of biopropanols from glycerol, both in batch and fixed bed reactors. Previous research by Zhu et al. [26] on liquid phase glycerol hydrogenolysis to 1-propanol and 2-propanol over Pt-$H_4SiW_{12}O_{40}$/ZrO_2 bifunctional catalysts at 200 °C and 5 MPa H_2 pressure revealed that appropriate metal-acid balance is important to promote the double dehydration-hydrogenation ability of glycerol. In our earlier study [27], we have explored the effect of different heteropolyacids on the glycerol conversion and selectivity to propanols by using a Pt-HPA/ZrO_2 catalytic system and a continuous flow, fixed-bed reactor set-up under ambient pressure. It was found that the metal dispersion and acidity of the catalyst attributed to the high activity. Lin et al. [28] reported the combined use of zeolite and Ni-based catalysts as a sequential two-layer catalyst system and achieved good selectivity of 1-propanol in a fixed-bed reactor.

Despite significant research efforts, most of the reported processes were energy intensive, requiring high hydrogen pressures and the use of organic solvents for the glycerol hydrogenolysis reaction, thus making the process unsustainable. In addition, the conversion of glycerol and selectivities to propanols are still not satisfied with these catalytic systems. Besides, the exact relation between the catalyst acidity and selectivity to propanols in glycerol hydrogenolysis needs to be properly elucidated. Hence, there is a large scope to improve the sustainability of the reaction process by making it energy efficient and increasing the process profitability. It is also most important to find a highly stable, active, and selective catalytic system that favors the production of propanols by one step hydrogenolysis of glycerol under ambient reaction conditions.
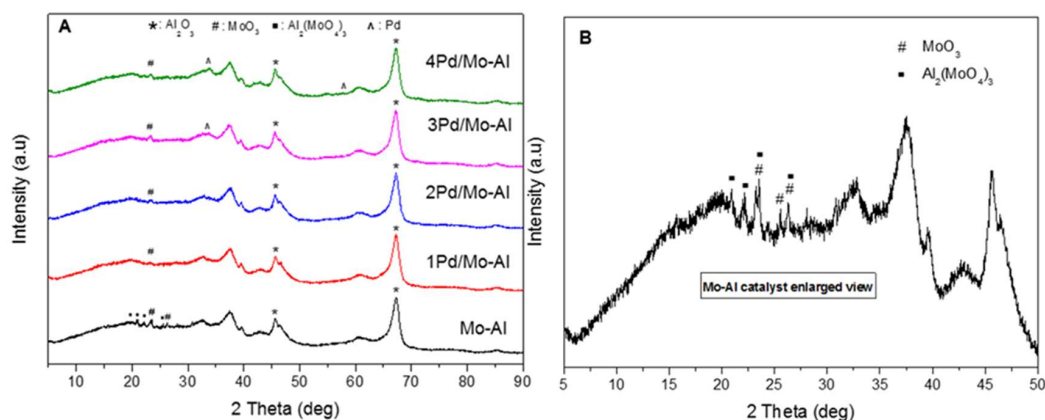
In the present investigation, we report a viable catalytic strategy for the direct hydrogenolysis of low-cost glycerol to valued bio propanols over bi-functional Pd/MoO_3-Al_2O_3 catalysts in a fixed-bed reactor without using an organic solvent. A series of 1–4 wt% $Pd/10\%MoO_3$-Al_2O_3 catalysts were prepared, carefully characterized by different characterization techniques, and tested in vapor phase glycerol hydrogenolysis at moderate temperature and atmospheric pressure. The effect of reaction parameters on the catalytic activity was investigated to determine the optimized reaction conditions. The stability of the catalyst has been analyzed to understand the changes in the catalytic activity. The research work reported herein contributes to the development of sustainable biodiesel industry, with the successful first use of alumina-supported palladium-molybdenum catalysts for the glycerol hydrogenolysis to propanols.

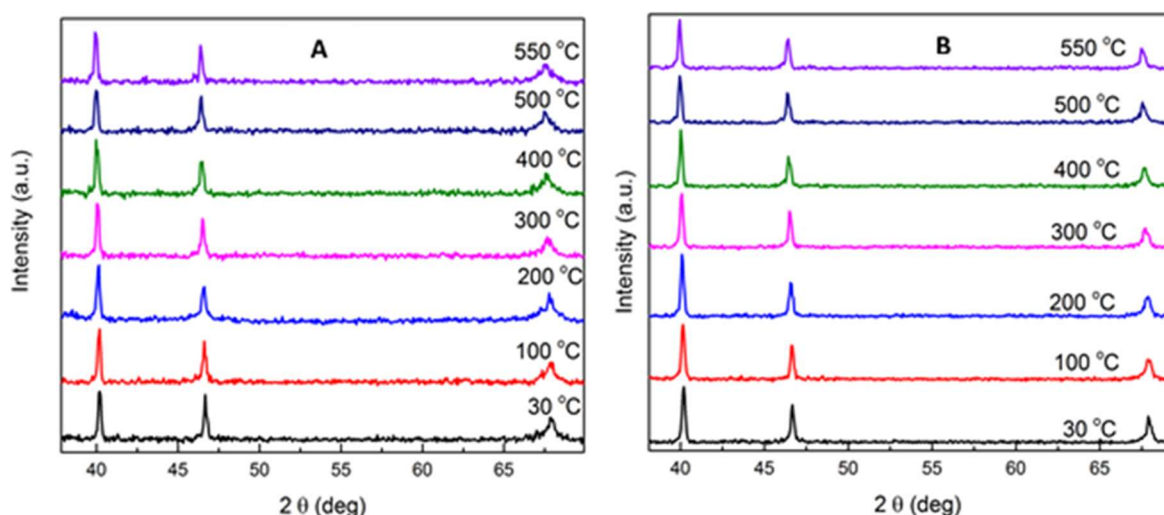## 2. Results and Discussion

2.1. Characterization Techniques

2.1.1. Structural Characterizations of the Catalysts

The X-ray Diffraction (XRD) patterns of Mo-Al and Pd/Mo-Al catalysts with various palladium contents (1–4 wt%) are shown in Figure 1A, and Figure 1B shows the enlarged view XRD pattern of Mo-Al catalyst. For all catalysts, the diffraction peaks of γ-Al_2O_3 were identified at 2θ = 45.8° and 67.1° [29] while the peaks at 2θ = 23.4° and 25.7° were assigned to the crystalline MoO_3 phase [30]. In addition, other peaks at 2θ = 20.7°, 22.0°, 23.4°, and 25.7° were identified, which are attributed to the $Al_2(MoO_4)_3$ phase. After the palladium addition, the characteristic diffraction peaks of MoO_3 and $Al_2(MoO_4)_3$ were found to be diminished. This indicates the better dispersion of MoO_3 on γ-Al_2O_3 in amorphous form and saturated monolayer coverage on the catalyst surface. Also, a peak at 2θ = 33° and 59° [31] corresponding to PdO was detected, which was found to be significant at higher Pd loadings and indicates fine dispersion at lower loadings.

Figure 1. (**A**) X-ray Diffraction (XRD) patterns of Mo-Al and various Pd/Mo-Al catalysts (**B**) XRD patterns of Mo-Al catalyst in the enlarged view.
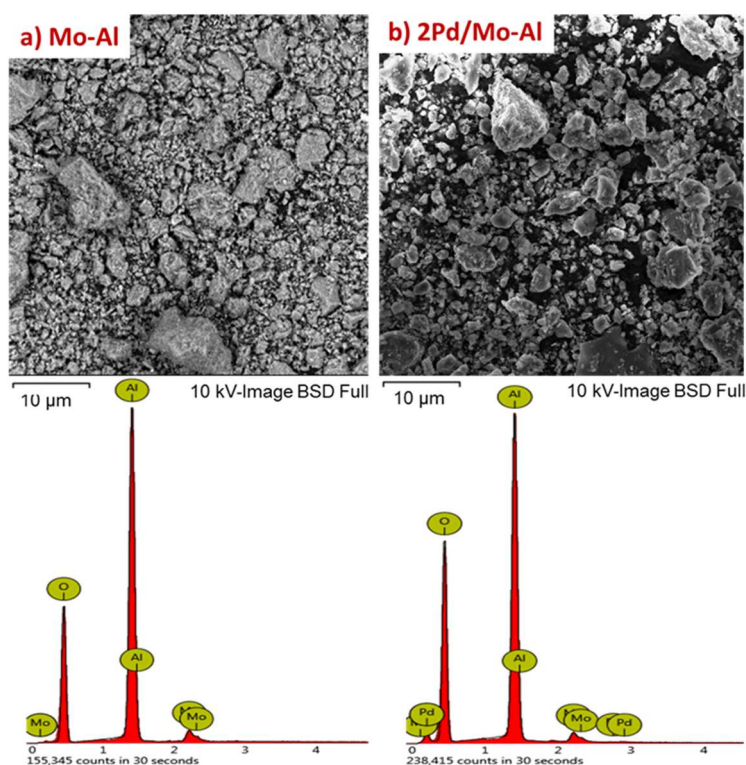
High-temperature X-ray diffraction (HTXRD) of MoO_3/Al_2O_3 support and dried $2Pd/MoO_3-Al_2O_3$ catalysts (the best catalytic system for this process) has been performed at various temperatures up to 550 °C to understand the nature of Pd interaction with the support during calcination, and its role in controlling the catalyst activity. As shown in Figure 2, There were not many significant changes in the XRD patterns of MoO_3/Al_2O_3 support at different temperatures, which clearly indicate the stability of the support at calcination temperature. The peaks appeared at $2\theta = 40°$, 46°, and 67° were assigned to the (hkl) crystalline phases of orthorhombic MoO_3/Al_2O_3. However, the HT-XRD patterns of the dried $2Pd/MoO_3-Al_2O_3$ at different temperatures were found to be slightly different as compared to the HT-XRD profiles of the support. The absence of any diffraction patterns corresponding to metallic Pd indicated that there was no formation of metallic Pd on the support. Relative intensities of the peak, as well as the peak width of these three peaks, corresponding to the support, showed slight changes, which usually happens when a metal ion like Pd is part of the $MoO_3-Al_2O_3$ crystalline framework. The XRD analysis performed at various temperatures, therefore, enabled us to test the stability of the catalysts and to determine the structure of the catalysts at different temperatures varying from room temperature to 550 °C.

Figure 2. High-temperature X-ray diffraction (HTXRD) patterns of (**A**) uncalcined Mo-Al and (**B**) 2Pd/Mo-Al catalysts.

Scanning electron micrographs (SEM) were acquired to study the topographical morphology of Mo-Al and 2 wt% Pd/Mo-Al catalysts. The semi-quantitative elemental analysis of the catalysts was performed by Scanning Electron Microscopy (SEM) coupled with Energy Dispersive X-ray spectroscopy (EDX). The SEM images and EDX profiles of Mo-Al and 2Pd-Mo-Al catalysts are displayed in Figure 3. As can be seen from Figure 3, the micrographs reveal crystalline aggregates of MoO_3 on γ-Al_2O_3 with a monolayer coverage. In the case of 2Pd/Mo-Al catalyst, both dense and less dense regions of bigger crystallites, along with highly dispersed palladium indicating a good coverage on the support [32], was observed.

The elemental analysis data for Mo-Al and various loadings of Pd/Mo-Al catalysts are presented in Table 1. Al_2O_3 was found to be the major component, with nearly similar atomic percentage of molybdenum in all the catalysts. All Pd/Mo-Al catalysts with varying Pd content (1–4 wt%) showed the presence of palladium, indicating the impregnation of palladium onto MoO_3/Al_2O_3 catalysts. The atomic percentages of Mo and Pd from SEM-EDX results were found to be consistent with the actual loadings used in the catalyst preparation. For a comparison, the Pd contents in a series of 1–4 wt% Pd/Mo-Al catalysts was measured by Inductive Coupled Plasma-Atomic Emission Spectrometer (ICP-AES), and the results are presented in Table 1.

Figure 3. Scanning electron micrograph (SEM) images of Mo-Al and 2 wt% Pd/Mo-Al catalysts.

Table 1. Energy Dispersive X-ray spectroscopy (EDX) and Inductive Coupled Plasma-Atomic Emission Spectrometer (ICP-AES) analysis data of Mo-Al, and various Pd/Mo-Al catalysts.

Catalyst	Weight Percentage (%) [a]					ICP-AES [b] (wt%)
	Mo	**Al**	**O**	**Pd**	**N**	
Mo-Al	7.83	48.17	44.00	–	–	–
1Pd/Mo-Al	6.99	43.02	48.82	0.67	0.50	0.59
2Pd/Mo-Al	7.12	40.86	50.22	1.22	0.58	1.18
3Pd/Mo-Al	7.01	40.33	49.70	2.41	0.55	2.20
4Pd/Mo-Al	7.24	40.99	48.21	3.07	0.49	2.97

[a] Determined from SEM-EDX analysis; [b] Metal contents determined from ICP-AES analysis.

2.1.2. Physicochemical Properties of Catalysts

The N_2 physisorption results of Mo-Al and various Pd/Mo-Al catalysts are listed in Table 2. The pure Mo-Al catalyst exhibited a total surface area of 189 m^2/g, with a pore diameter of 5.9 nm. After incorporation of palladium into catalysts, the Brunauer–Emmett–Teller (BET) surface area, the average pore volume, and the pore size of all catalysts were found to be smaller than the original Mo-Al catalyst. This change is obvious because of the impregnation of Pd on the support that would block the micropores of the catalysts [30].

Table 2. Physicochemical properties of Mo-Al and various Pd/Mo-Al catalysts.

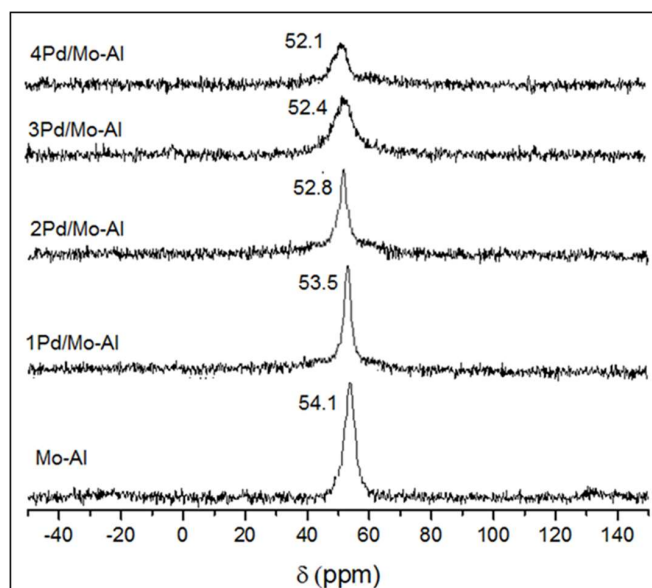| Catalyst	BET Surface Area (m^2/g)	Pore Size (nm)	Pore Volume (cm^3/g)
Mo-Al	189	5.9	0.29
1Pd/Mo-Al	181	5.8	0.28
2Pd/Mo-Al	170	5.6	0.28
3Pd/Mo-Al	162	5.3	0.26
4Pd/Mo-Al	158	5.3	0.23

2.1.3. Acidity Measurement by NH$_3$–TPD Analysis

Temperature programmed desorption (TPD) experiments of γ-Al$_2$O$_3$, Mo-Al and 1–4 wt% Pd/Mo-Al catalysts were performed to determine the amount and strength of acid sites. The number of acid sites calculated from the desorption TPD peak area is presented in Table 3. Agreeing with the literature [33], three ranges of NH$_3$ desorption temperature should be taken into account: 50–200, 200–350, and 350–550 °C, which correspond to weak, moderate, and strong acid sites, respectively. The pure γ-Al$_2$O$_3$ catalyst exhibited weak to moderate acidity in the temperature regions of 150–350 °C. The total acidity decreased with the addition of Mo, with a significant decrease in moderate acid sites. This could be due to a decrease in surface area and blockage of acidic sites of γ-Al$_2$O$_3$. After incorporation of Pd in Mo-Al catalyst, weaker to moderate acid sites remained in all catalysts, with no generation of new acid sites. However, it is to be noted that there was an increase in the moderate acid site in all Pd loaded catalysts compared to Mo-Al catalyst. This indicates that weak to moderate acid centers of catalyst had a crucial role in facilitating the glycerol hydrogenolysis reaction.

Table 3. Acidities of γ-Al$_2$O$_3$, Mo-Al, and 1–4 wt% Pd/Mo-Al catalysts from Temperature programmed desorption of ammonia (NH$_3$-TPD) analysis.

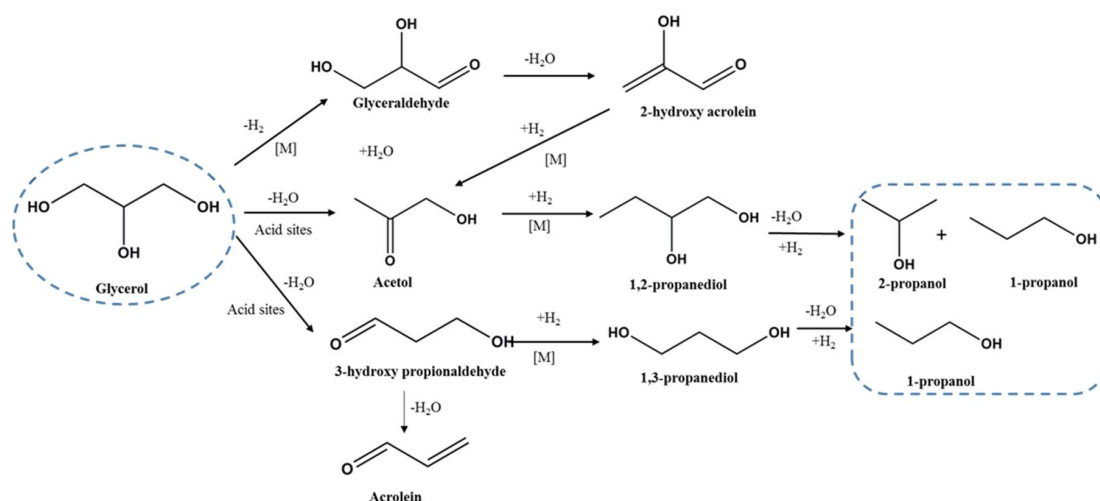| Catalyst	NH$_3$ Uptake (µmol/g)			Total NH$_3$ Uptake (µmol/g)
	Weak	Moderate	Strong	
γ-Al$_2$O$_3$	298.7	426.2	–	724.9
Mo-Al	323.5	350.6	–	674.1
1Pd/Mo-Al	297.3	361.2	–	658.5
2Pd/Mo-Al	273.3	372.2	–	645.5
3Pd/Mo-Al	194.2	369.0	–	563.2
4Pd/Mo-Al	195.0	364.9	–	559.9

2.1.4. ^{27}Al NMR Spectroscopy

Solid state ^{27}Al nuclear magnetic resonance (NMR) spectroscopy is a non-invasive and non-destructive technique vital to studying the structural modifications and coordination of aluminium nuclei within the catalyst subjected to impregnation and calcination. The chemical analysis and comparison of ^{27}Al NMR spectra of Mo-Al and 1–4 wt% Pd/Mo-Al catalyst samples is presented in Figure 4. The spectrum of Mo-Al consists of a single peak at a chemical shift of 54.1 ppm from octahedral aluminium, characteristic of as-prepared catalysts. Similar results were obtained for all the Pd/Mo-Al catalysts, indicating that palladium impregnation did not alter the basic aluminium framework. However, upon impregnation of palladium onto Mo-Al catalyst, it was observed that there was a slight change in the chemical shift of octahedral Al peak. At higher loadings, the peak was markedly broadened, and the intensity of the peak was decreased. This is probably due to the palladium interaction with the support material that causes the expulsion or distortion of aluminium atoms from the framework sites [34].

Figure 4. ^{27}Al nuclear magnetic resonance (^{27}Al NMR) spectra of Mo-Al and 1–4 wt% Pd/Mo-Al catalysts.

2.2. Catalytic Studies

Glycerol hydrogenolysis is a complex reaction (Scheme 2) and is generally believed to proceed via dehydration-hydrogenation route in two distinct pathways, which involve the formation of intermediates (acetol and 3-hydroxypropanaldehyde (3-HPA)) by acid-catalyzed dehydration and subsequent formation of propanediols (1,2-PDO and 1,3-PDO) over metal sites [35–39]. Thereafter, C-O hydrogenolysis of 1,2-PDO results in the formation of 1-propanol (1-PrOH), while C-O hydrogenolysis of 1,3-PDO gives rise to 2-propanol (2-PrOH). Another possible pathway is the formation of glyceraldehyde and 2-hydroxy acrolein by the dehydrogenation-dehydration-hydrogenation mechanism, in which acetol can be indirectly formed by this pathway. Direct hydrogenolysis of glycerol to propanols in one step using a single catalyst, though highly challenging, would be consistent and more preferential over a two-step process in terms of energy efficiency.
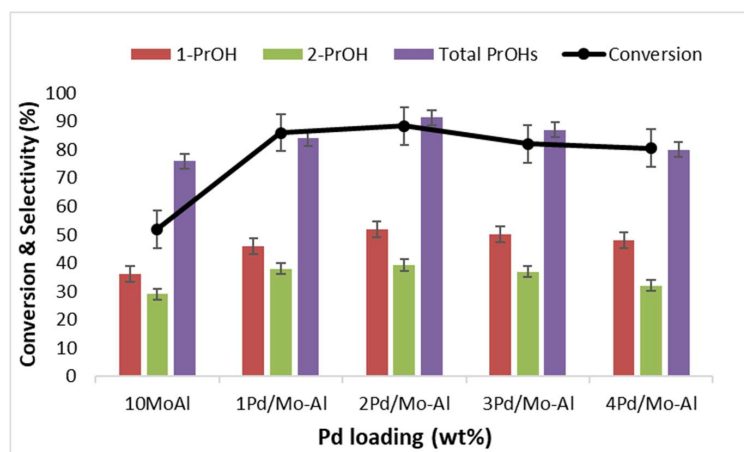

Scheme 2. Series and parallel network of reactions in hydrogenolysis of glycerol.

The present work focused on the investigation of hydrogenolysis of glycerol over highly efficient Pd/MoO$_3$-Al$_2$O$_3$ catalysts with various Pd loadings (1–4 wt%) in a continuous flow, fixed-bed reactor at 210 °C under atmospheric pressure. The reaction successfully progressed to give propanols (1-PrOH

+ 2-PrOH) as major products. Interestingly, the presence of weak to moderates acid sites in the Pd/Mo-Al catalyst promoted the double dehydration and hydrogenation of glycerol to 1-propanol and 2-propanol, respectively. Further analysis and optimization of the reaction process helped to achieve the best glycerol conversion and selectivity to propanols. Optimisation of the reaction process included adjusting various reaction parameters such as the effect of Pd loading, reaction temperature, and hydrogen flow rate. All Pd/Mo-Al catalysts showed good activity in terms of glycerol conversion and propanol selectivity in glycerol hydrogenolysis. However, the activity differed upon altering the reaction parameters, which facilitated determining the best catalyst that resulted in the highest activity.

2.2.1. Effect of Pd Loading

Defining the ideal metal loading of a catalyst for glycerol hydrogenolysis is important, as metal sites play a crucial role in the reaction mechanism. Therefore, the glycerol hydrogenolysis was performed using Pd/Mo-Al catalysts with varying Pd loading (1–4 wt%), and the results obtained are presented in Figure 5. In the absence of palladium over 10 wt% MoO_3-Al_2O_3, only about 52% glycerol conversion was observed, with 76% selectivity to total propanol. The incorporation of Pd into the catalyst resulted in significant increase in the glycerol conversion and product selectivity. As can be seen from Figure 5, a maximum of 88.4% glycerol conversion with a 91.3% selectivity to total propanol was attained over 2 wt% Pd catalyst. Further, increase in Pd loading to 3 and 4 wt% showed a drop in activity, which concludes that 2 wt% Pd/Mo-Al catalyst with an appropriate number of Pd sites influenced the direct hydrogenolysis of glycerol to propanols. Thus, 2 wt% Pd catalyst has been chosen to be the optimal catalyst for further investigations.
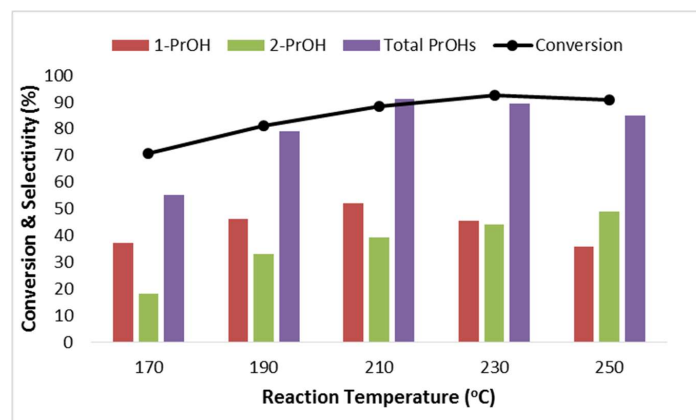

Figure 5. Effect of Pd loading on glycerol hydrogenolysis to propanols. Reaction conditions: Reaction temperature: 210 °C, 0.1 MPa H_2; H_2 flow rate: 100 mL/min; 10 wt% aqueous glycerol; 0.5 g catalyst; Reaction time: 6 h; 1-PrOH: 1-propanol; 2-PrOH: 2-Propanol; Total PrOHs: Total propanol.

2.2.2. Effect of Reaction Temperature

To assess the influence of reaction temperature on glycerol conversion and propanol selectivity, the glycerol hydrogenolysis reaction was performed over 2 wt% Pd/Mo-Al catalyst at different reaction temperatures going from 170 to 250 °C, and the results are shown in Figure 6. It is obvious that the reaction temperature had a positive influence on the glycerol conversion, as suggested by previous studies [40,41]. With the increase in the temperature from 170 °C to 230 °C, the glycerol conversion increased steadily from 70.6% up to 92.6%. The highest total propanol selectivity of 91.3% was obtained at a reaction temperature of 210 °C. Further increase of temperature to 250 °C caused a decrease in glycerol conversion and 1-PrOH selectivity. However, it is noteworthy that the selectivity to 2-PrOH elevated at a higher temperature. Therefore, the results suggest that a reaction temperature of 210 °C promoted excessive C-O hydrogenolysis of glycerol to produce the highest amounts of 1-propanol and
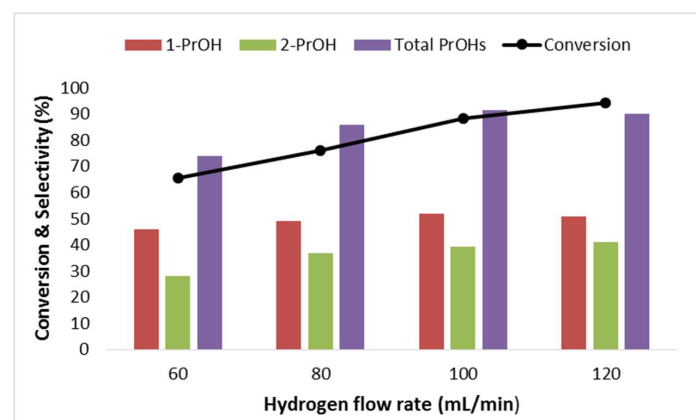
2-propanol, in addition to confirming that reaction temperature had a significant effect on the product distribution of 1-PrOH and 2-PrOH.

Figure 6. Effect of Reaction temperature on glycerol hydrogenolysis to propanols. Reaction conditions: Reaction temperature = 170–250 °C, Reduction temperature = 350 °C; 0.1 MPa H_2; H_2 flow rate = 100 mL/min; 10 wt% aqueous glycerol; 0.5 g catalyst; Reaction time: 6 h; 1-PrOH: 1-propanol; 2-PrOH: 2-Propanol; Total PrOHs: Total propanols.

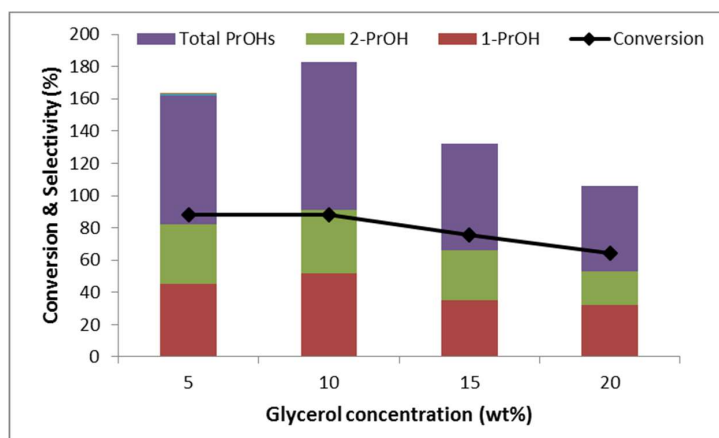### 2.2.3. Effect of Hydrogen Flow Rate

Hydrogen is a key reactant in hydrogenolysis reaction, and it is important to understand the influence of the hydrogen flow rate on glycerol hydrogenolysis. Optimising the hydrogen flow rate will add value to the process and will balance the higher costs of high-pressure apparatus. Hence the reaction was investigated by varying the hydrogen pressures at 60, 80, 100, and 120 mL/min over 2 wt% Pd/Mo-Al catalyst at 210 °C under atmospheric pressure. As can be observed from Figure 7, the glycerol conversion and selectivity of 1-PrOH increased with an increase in hydrogen flow rate from 60 to 120 mL/min. However, the total PrOH selectivity was found to be the highest at a hydrogen flow rate of 100 mL/min. While when the hydrogen flow rate was 120 mL/min, total PrOH selectivity slightly dropped, in spite of distinct increment in glycerol conversion, to 94%. This is probably because at higher hydrogen flow rates excessive hydrogenolysis occurs, leading to the formation of degradative products. A similar observation was made in previous studies [42]. Thus, 100 mL/min hydrogen flow rate was considered to be optimum for this reaction, resulting in a maximum total PrOHs selectivity of 91.3% at 88.4% glycerol conversion.

Figure 7. Effect of Hydrogen flow rate on glycerol hydrogenolysis to propanols. Reaction conditions: Reaction temperature = 210 °C; H_2 flow rate = 60, 80, 100 & 120 mL/min, 0.1 MPa H_2; 10 wt% aqueous glycerol; 0.5 g catalyst; Reaction time: 6 h; 1-PrOH: 1-propanol; 2-PrOH: 2-Propanol; Total PrOHs: Total propanols.
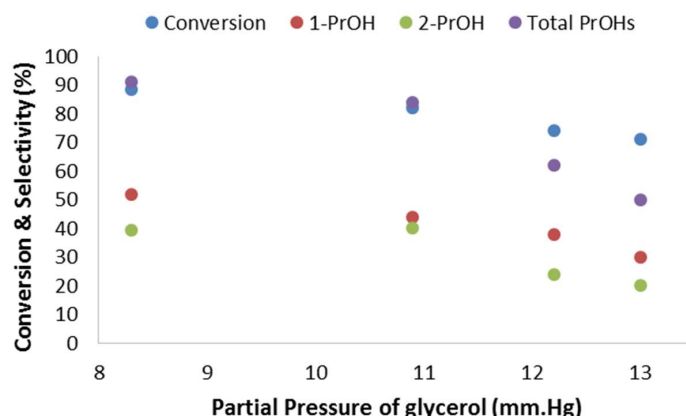
2.2.4. Effect of Glycerol Concentration

The glycerol concentration serves as one of the most important parameters which has a significant effect on the activity and selectivity of glycerol hydrogenolysis reaction. It is known that a low concentration of glycerol is favorable to increase the glycerol conversion [17,43]. Figure 8 shows the activity results at different glycerol concentrations (5–20 wt%), which was performed over 2 wt% Pd/Mo-Al catalyst to identify the best activity. From the results, it was observed that by increasing the glycerol concentration from 5 wt% to 20 wt%, both the glycerol conversion and selectivity to total propanols declined. As the glycerol content increased, the glycerol conversion and the selectivity towards propanols decreased considerably. With 5 wt% glycerol feed, 88% of glycerol converted, with about 80% selectivity to total propanols. At 10 wt% glycerol feed, the selectivity to total propanols was improved to 91.3% at nearly the same glycerol conversion, indicating the excessive hydrogenolysis of glycerol to propanols. At higher glycerol concentration (15 and 20 wt%), it was observed that both conversion and selectivity dropped considerably, which is ascribed to the fact that the reaction rate is lowered due to high viscosity of the glycerol feed and the imbalance between the catalytically active sites and the excess glycerol available to react at higher concentrations. Consequently, 10 wt% glycerol feed was considered the optimal concentration to attain the highest glycerol conversion of glycerol and selectivity to total propanols.

Figure 8. Effect of glycerol concentration on glycerol hydrogenolysis to propanols. Reaction conditions: Reaction temperature = 210 °C; H_2 flow rate = 100 mL/min, 0.1 MPa H_2; 5–10 wt% glycerol feed; 0.5 g catalyst; Reaction time: 6 h; 1-PrOH: 1-propanol; 2-PrOH: 2-Propanol; Total PrOHs: Total propanols.

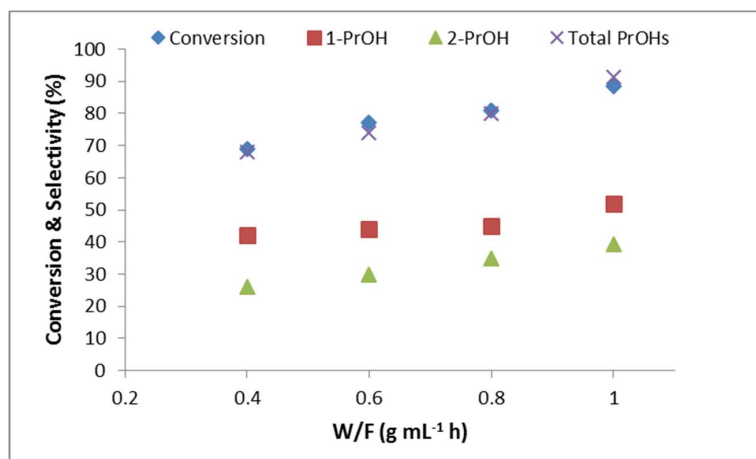### 2.2.5. Effect of the Partial Pressure of Glycerol

Figure 9 shows the effect of partial pressure of glycerol on glycerol conversion, and total propanols selectivity for the 2 Pt/Mo-Al catalyst at 210 °C, 100 mL/min H_2 flow rate, 10 wt% glycerol solution, and at different glycerol feed flow rates of 0.5, 1.0, 1.5, and 2.0 mL/h. With the increase in partial pressure of glycerol from 8.3–13.0 mm Hg, the conversion of glycerol decreased from 88.4% to 71%, and the selectivity to total propanols decreased almost two-fold. This decrease in conversion and selectivity can be attributed to a decrease in the number of active sites due to the increase in the flow of glycerol feed [44].

Figure 9. Effect of the partial pressure of glycerol on glycerol hydrogenolysis to propanols. Reaction conditions: Reaction temperature = 210 °C; H_2 flow rate = 100 mL/min, 0.1 MPa H_2; 10 wt% aqueous glycerol; 0.5, 1.0, 1.5 and 2.0 mL/h glycerol feed; 0.5 g catalyst; Reaction time: 6 h; 1-PrOH: 1-propanol; 2-PrOH: 2-Propanol; Total PrOHs: Total propanols.

2.2.6. Effect of Contact Time (W/F)

The dependence of the rate of glycerol hydrogenolysis on contact time (W/F) in the range of 0.4 to 2.0 g mL^{-1} h at 210 °C, 0.5 mL/h 10 wt% glycerol feed was studied over 2Pd/Mo-Al catalyst by varying the weight of the catalyst. As can be noted from Figure 10, the glycerol conversion increases steadily from 60% to 88.4% with an increase in the contact time. Similarly, the selectivity to total propanols was also found to increase substantially from 68% to 91.3% upon increasing the contact time. This observation suggests that greater contact time enables the strong adsorption of glycerol on to the catalytically active sites and facilitates the excessive hydrogenolysis reaction of glycerol to produce double dehydration-dehydrogenation products 1-propanol and 2-propanol, which is in good agreement with the previous studies [27].
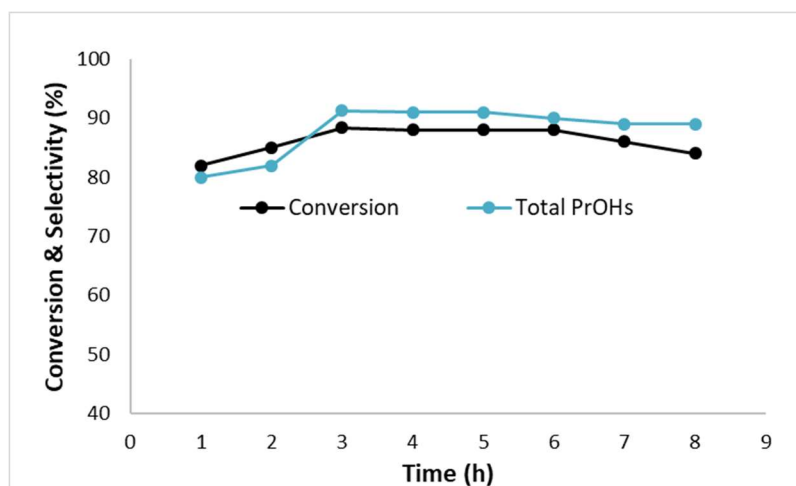

Figure 10. Effect of contact time on glycerol hydrogenolysis to propanols. Reaction conditions: Reaction temperature = 210 °C; H_2 flow rate = 100 mL/min, 0.1 MPa H_2; 10 wt% aqueous glycerol; 0.5 mL/h glycerol feed; 0.2–0.5 mg catalyst; Reaction time: 6 h; 1-PrOH: 1-propanol; 2-PrOH: 2-Propanol; Total PrOHs: Total propanols.

From all the above sequence of experiments, the optimal set of reaction conditions to accomplish the best possible glycerol conversion and total propanols selectivity over 2Pd/Mo-Al catalyst were identified as 210 °C, 100 mL/min H_2 flow rate, 10 wt% glycerol concentration, 8.3 mm Hg partial pressure of glycerol, and at 1.0 g mL^{-1} h contact time. Under these best set of conditions, the most active 2Pd/Mo-Al catalysts was tested for stability and reusability, and the results are analyzed.

2.2.7. Time on Stream Experiment

Time on stream experiment for 8 h was conducted over the best catalyst 2 wt% Pd/Mo-Al under the similar reaction conditions to investigate the stability and activity of catalyst (Figure 11). The conversion of glycerol progressively increased from 82% and reached a maximum of 88.4% at 3 h and remained constant up until 6 h. Also, the selectivity to total PrOH also maximized at 3 h, remained the same until 5 h, and presented a slight decline during 6–8 h. This decline in activity might be probably due to the fact that the catalyst suffers slow deactivation during the reaction due to carbon deposition. A similar finding was reported in our previous studies [8,35].
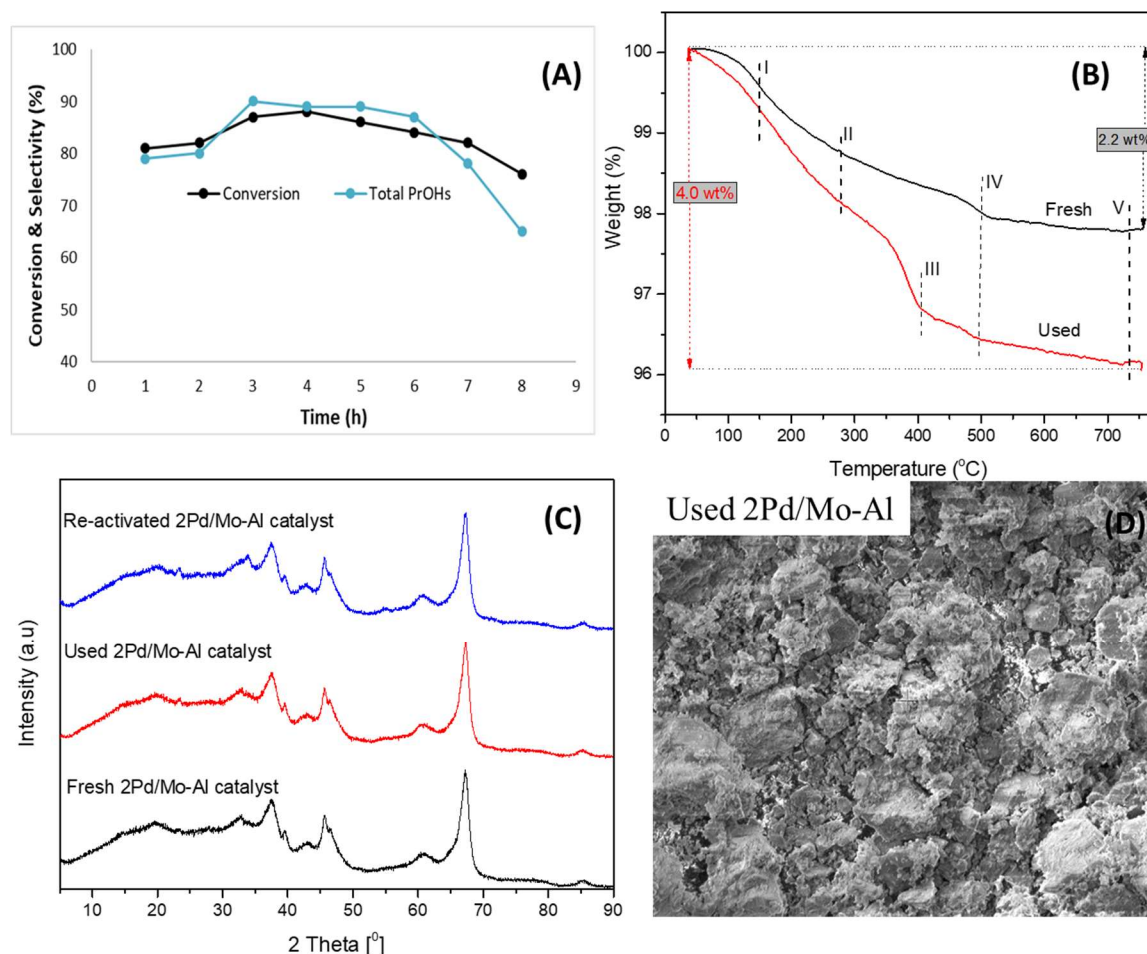

Figure 11. Time-on-stream experiment over fresh 2 wt% Pd/Mo-Al$_2$O$_3$ catalyst. Reaction conditions: Reaction temperature = 210 °C; 0.1 MPa H$_2$; H$_2$ Flow rate = 100 mL/min, 10 wt% aqueous glycerol; 0.5 g catalyst; Total PrOHs: Total propanols.

2.3. Reusability of the Catalyst

To further understand the stability and reusability of catalyst, the spent 2Pd/Mo-Al catalyst was regenerated by activating the catalyst in air flow (100 mL/min) at 500 °C for 2 h and then tested in glycerol hydrogenolysis time-on-stream experiment under the similar reaction conditions used for the fresh catalyst. The performance of 2Pd/Mo-Al catalyst upon re-use is illustrated in Figure 12A. The results were reproduced over the used catalyst and demonstrated a similar pattern to that of the fresh catalyst during 1–6 h. However, there is a slight decline in glycerol conversion and a significant drop in the selectivity to total propanols at later hours. The cause for the decrease in activity might be due to the catalyst deactivation over time due to agglomeration or carbon deposition. The used and reactivated catalysts were further analyzed by various characterization techniques, and the results are presented in Table 4 & Figure 12.

Table 4. Studies on the used 2Pd/Mo-Al catalyst.

Catalyst	Conversion (%)	Selectivity of Total PrOHs (%)	BET Surface Area (m^2/g)	Total Acidity (NH$_3$ µmol/g)
Fresh	88.4	91.3	170	645.5
Used	87.0	90.0	162	594.0
Reactivated	88.0	90.9	168	617.2

Figure 12. (**A**) Time-on-stream experiment over used 2 wt% Pd/Mo-Al catalyst; (**B**) thermogravimetric analysis (TGA) profile of fresh and used catalyst; (**C**) XRD pattern of fresh, used and reactivated catalyst; (**D**) SEM image of used 2Pd/Mo-Al catalyst.

The XRD pattern, SEM image, BET SA, and total acidity from NH_3-TPD analysis of the used 2Pd/Mo-Al catalyst showed no significant changes, indicating that the catalytic structure remained intact during the course of the reaction. Thermogravimetric analysis (TGA) was used to characterize the used catalyst to understand the mode of deactivation. The TGA measurements were performed over a temperature range of 50 °C to 750 °C at a heating rate of 10 °C/min under a constant flow of nitrogen (20 mL/min). The recorded TG curves of fresh and used catalysts presented as Figure 12B consist of four mass loss processes common in both fresh and used catalysts and an additional mass loss process observed in used catalyst. The first step (I) between 100 and 130 °C corresponds to removal of physisorbed water; the second mass loss region (II) around 250 °C indicates the loss of coordinated water molecules; the fourth weight loss step (IV) between 450–500 °C is attributed to the removal of strongly bound hydroxyl groups from alumina matrix; and a small weight loss (V) above 700 °C is due to the sublimation of molybdena [45]. In addition, a large weight loss region (III) extended above 380–500 °C in the used catalyst corresponds to the loss of carbonaceous materials [46], indicating the deactivation of the catalyst by carbon deposition. The total weight loss due to heating at the temperature range 50–750 °C for the used catalyst was found to be 4.0 wt% while it was just 2.2 wt% for the fresh catalyst, which clearly indicates that the excess weight loss is due to the deposition of carbon species and undesired materials on the catalyst surface during the reaction.

3. Materials and Methods

3.1. Catalyst Preparation

A series of palladium catalysts on 10 wt% MoO_3/Al_2O_3 with varying palladium loading from 1.0–4.0 wt% was prepared by wet impregnation method. Tetraammine palladium (II) nitrate solution (10 wt% in H_2O, produced by Sigma Aldrich Co., Ltd., St. Louis, MO, USA) was used as a precursor on the support. 10 wt% MoO_3/Al_2O_3 (2–5 mm pellets) was obtained from Riogen. The prepared catalysts were dried overnight at 100 °C and subsequently calcined at 500 °C for 2 h in air. The prepared catalysts were labelled as xPd/Mo-Al, where x refers to Pd loading, Mo refers to MoO_3, and Al refers to Al_2O_3.

3.2. Catalyst Characterization

The X-ray Diffraction (XRD) of catalysts was performed on a Miniflex X-ray diffractometer (Rigaku, Neu-Isenburg, Germany) with Ni-filtered Cu-Kα radiation (λ = 1.392 Å). The angles of scanning were from 2° to 90° with a rate of 2°/min, with the beam voltage and a beam current of 30 kV and 15 mA, respectively. High Temperature X-ray diffraction (HTXRD) profiles of the catalysts as a function of temperature were carried out using Bruker D8 Advance X-ray diffractometer equipped with the Anton-Parr heating accessory.

Nitrogen physisorption analysis of the catalysts was carried at −196 °C under liquid N_2 with a Quantachrome Autosorb 1 instrument. As a pretreatment of the N_2 physisorption analysis, each catalyst sample is degassed under vacuum for 6 h at 250 °C. The multi-point Brunauer–Emmet–Teller (BET) method was used to calculate the specific surface areas of each catalyst and the Barrett–Joyner–Halenda model (BJH) method was used to measure the average pore diameter and pore volumes.

Scanning electron microscopy (SEM) was used to study the morphology of the catalyst samples, and the elemental identification of the catalysts was performed by Energy Dispersive X-Ray Analyzer coupled to Phenom XL scanning electron microscopy (SEM-EDX). Before analysis by SEM, each sample was mounted on an aluminum support using double adhesive carbon tape. At 10 kV beam voltage and 5000× magnification, the micrographs of the catalysts were captured using a backscatter electron detector (BSD). The elemental analysis was performed at high resolution (15 kV of beam voltage) and high vacuum pressure (1 Pa) with a secondary electron detector (SED), where the point and mapping analysis for element identification was performed using a Phenom Pro Suite software.

The amount of Pd in all Pd/Mo-Al catalysts was quantitatively analyzed by Inductively coupled plasma atomic emission spectrometry (Agilent Technologies-4200MP-AES, Santa Clara, CA, USA). The samples were prepared by acid digestion of catalyst (~10 mg in 2 mL aquaregia) at 60 °C followed by dilution to desired concentration.

Temperature programmed desorption of ammonia (NH_3-TPD) experiments were conducted on AutoChem 2910 (Micromeritics, Norcross, GA, USA) instrument. In a typical experiment, 100 mg of oven-dried sample was pretreated by passage of high purity (99.995%) helium (50 mL min^{-1}) at 200 °C for one hour. After pretreatment, the sample was saturated with highly pure anhydrous ammonia (50 mL min^{-1}) with a mixture of 10% NH_3–He at 80 °C for 1 h and subsequently flushed with He flow (50 mL min^{-1}) at 80 °C for 30 min to remove physisorbed ammonia. TPD analysis was carried out from ambient temperature to 700 °C at a heating rate of 10 °C min^{-1}. The amount of NH_3 desorbed was calculated using the GRAMS/32 software.

Solid state ^{27}Al Nuclear Magnetic Resonance Spectroscopy (^{27}Al NMR) technique was used to identify the basic aluminium framework structure of catalysts on DD2 Oxford Magnet AS-500MHz spectrometer (Agilent Technologies) using aluminium oxide (Aldrich) as a probe. The chemical shifts (δ) are revealed in ppm.

Thermo gravimetric analysis (TGA) was performed using a Perkin Elmer TGA-7 from 35 °C to 700 °C with a heating rate of 10 °C per minute under the flow of nitrogen.

3.3. Catalyst Testing

The glycerol hydrogenolysis experiments were conducted in the vapour phase under atmospheric pressure in a vertical fixed bed quartz reactor (40 cm length, 9 mm i.d.) using 0.5 g of catalyst. Before the reaction, the catalysts were pretreated at 350 °C for 2 h in flowing H_2 (60 mL min^{-1}). After cooling down to the reaction temperature (210 °C), an aqueous solution of 10 wt% glycerol was introduced into the reactor using a feed pump along with the flow of hydrogen (100 mL/min). The reaction products were condensed in an ice–water trap and collected hourly for analysis on a gas chromatograph GC-2014 (Shimadzu, Kyoto, Japan) equipped with a DB-wax 123-7033 (Agilent) capillary column (0.32 mm i.d., 30 m long) and flame ionization detector. The conversion of glycerol (1) and selectivity (2) of products were calculated as follows:

$$Conversion\ (\%) = \frac{moles\ of\ glycerol\ (in) - moles\ of\ glycerol\ (out)}{moles\ of\ glycerol\ (in)} \times 100$$

$$Selectivity\ (\%) = \frac{moles\ of\ one\ product}{moles\ of\ all\ products} \times 100$$

4. Conclusions

A simple and highly efficient protocol of direct hydrogenolysis of glycerol to 1-propanol and 2-propanol over a series of 1–4 wt% Pd/MoO$_3$-Al$_2$O$_3$ catalysts has been demonstrated. Pd/Mo-Al catalysts were prepared by wetness impregnation method and characterized by XRD, SEM, NH$_3$-TPD, ^{27}Al NMR, and BET to evaluate the physical and chemical properties of catalysts. The hydrogenolysis of glycerol was performed in vapour phase under atmospheric pressure. Among the catalysts tested, 2 wt% Pd/Mo-Al catalyst established high activity and selectivity in the glycerol hydrogenolysis, with 91.3% total propanol selectivity at 88.4% glycerol conversion at best reaction conditions of 210 °C, 1 bar pressure, 100 mL/min H$_2$ flow rate, 10 wt% aq. Glycerol, and 8.3 mm Hg partial pressure of glycerol. The weak to moderate acidity of the catalyst was found to affect the degree of glycerol dehydroxylation, and promoted double dehydration of glycerol to form 1-propanol and 2-propanol. A comprehensive study on reaction parameters revealed the optimized reaction conditions and it was found that the reaction temperature, partial pressure of glycerol, and contact time had a substantial influence on the glycerol conversion and propanol selectivity. Further, the time on stream studies demonstrated that the catalyst remained stable for a longer period without great loss in the conversion and selectivity to products. The activity results were well correlated with the results obtained from catalyst characterization. The study signifies a sustainable technology that can not only develop the opportunity of biodiesel industry, but also deliver a green chemical production route from biomass-derived glycerol.

References

1. Werpy, T.; Petersen, G.; Aden, A.; Bozell, J.; Holladay, J.; White, J.; Manheim, A.; Eliot, D.; Lasure, L.; Jones, S. *Top Value Added Chemicals from Biomass. Results of Screening for Potential Candidates from Sugars and Synthesis Gas*; US Department of Energy: Southwest Washington, DC, USA, 2004; Volume 1.
2. Zhou, C.H.C.; Beltramini, J.N.; Fan, Y.X.; Lu, G.Q.M. Chemoselective catalytic conversion of glycerol as a biorenewable source to valuable commodity chemicals. *Chem. Soc. Rev.* **2008**, *37*, 527–549. [CrossRef] [PubMed]

3. Priya, S.S.; Selvakannan, P.R.; Chary, K.V.R.; Kantam, M.L.; Bhargava, S.K. Solvent-Free Microwave-Assisted Synthesis of Solketal from Glycerol Using Transition Metal Ions Promoted Mordenite Solid Acid Catalysts. *J. Mol. Catal. A Chem.* **2017**, *434*, 184–193. [CrossRef]

4. Li, R.; Song, H.; Chen, J. Propylsulfonic Acid Functionalized SBA-15 Mesoporous Silica as Efficient Catalysts for the Acetalization of Glycerol. *Catalysts* **2018**, *8*, 297. [CrossRef]

5. Bossaert, W.D.; De Vos, D.E.; Rhijn, W.M.V.; Bullen, J.; Grobet, P.J.; Jacobs, P.A. Mesoporous Sulfonic Acids as Selective Heterogeneous Catalysts for the Synthesis of Monoglycerides. *J. Catal.* **1999**, *182*, 156–164. [CrossRef]

6. Karinen, R.S.; Krause, A.O.I. New biocomponents from glycerol. *Appl. Catal. A Gen.* **2006**, *306*, 128–133. [CrossRef]

7. Demirel, S.; Lucas, M.; Warna, J.; Salmi, T.; Murzin, D.; Claus, P. Reaction kinetics and modeling of the gold catalysed glycerol oxidation. *Top. Catal.* **2005**, *44*, 299–305. [CrossRef]

8. Kim, Y.T.; Jung, K.D.; Park, E.D. Gas-phase dehydration of glycerol over ZSM-5 catalysts. *Microporous Mesoporous Mater.* **2010**, *131*, 28–36. [CrossRef]

9. Priya, S.S.; Kandasamy, S.; Bhattacharya, S. Turning Biodiesel Waste Glycerol into 1,3-Propanediol: Catalytic Performance of Sulphuric acid-Activated Montmorillonite Supported Platinum Catalysts in Glycerol Hydrogenolysis. *Nat. Sci. Rep.* **2018**, *8*, 7484.

10. King, D.L.; Zhang, L.; Xia, G.; Karim, A.M.; Heldebrant, D.J.; Wang, X.; Peterson, T.; Wang, Y. Aqueous phase reforming of glycerol for hydrogen production over Pt–Re supported on carbon. *Appl. Catal. B Environ.* **2010**, *99*, 206–213. [CrossRef]

11. Sun, D.; Yamada, Y.; Sato, S.; Ueda, W. Glycerol hydrogenolysis into useful C3 chemicals. *Appl. Catal. B Environ.* **2010**, *193*, 75–92. [CrossRef]

12. Unruh, J.D.; Pearson, D. *Kirk-Othmer Encyclopedia of Chemical Technology*; John Wiley & Sons: New York, NY, USA, 2000.

13. Logsdon, J.E.; Loke, R.A. *Kirk-Othmer Encyclopedia of Chemical Technology*; John Wiley & Sons: New York, NY, USA, 2000.

14. Dam, J.T.; Djanashvili, K.; Kapteijn, F.; Hanefeld, U. Pt/Al$_2$O$_3$ Catalyzed 1,3-Propanediol Formation from Glycerol using Tungsten Additives. *ChemCatChem* **2013**, *5*, 497–505.

15. Arundhathi, R.; Mizugaki, T.; Mitsudome, T.; Jitsukawa, K.; Kaneda, K. Highly Selective Hydrogenolysis of Glycerol to 1,3-Propanediol over a Boehmite-Supported Platinum/Tungsten Catalyst. *ChemSusChem* **2013**, *6*, 1345–1347. [CrossRef] [PubMed]

16. Zhu, S.; Qiu, Y.; Zhu, Y.; Hao, S.; Zheng, H.; Li, Y. Hydrogenolysis of glycerol to 1,3-propanediol over bifunctional catalysts containing Pt and heteropolyacids. *Catal. Today* **2013**, *212*, 120–126. [CrossRef]

17. Priya, S.S.; Kumar, V.P.; Kantam, M.L.; Bhargava, S.K.; Chary, K.V.R. Catalytic performance of Pt/AlPO$_4$ catalysts for selective hydrogenolysis of glycerol to 1,3- propanediol in the vapour phase. *RSC Adv.* **2014**, *4*, 51893–51903. [CrossRef]

18. Ryneveld, E.V.; Mahomed, A.S.; Heerden, P.S.V.; Green, M.J.; Friedrich, H.B. A catalytic route to lower alcohols from glycerol using Ni-supported catalysts. *Green Chem.* **2011**, *13*, 1819–1827. [CrossRef]

19. Tamura, M.; Amada, Y.; Liu, S.; Yuan, Z.; Nakagawa, Y.; Tomishige, K. Promoting effect of Ru on Ir-ReOx/SiO$_2$catalyst in hydrogenolysisof glycerol. *J. Mol. Catal. A Chem.* **2014**, *388–399*, 177–187. [CrossRef]

20. Furikado, I.; Miyazawa, T.; Koso, S.; Shimao, A.; Kunimori, K.; Tomishige, K. Catalytic performance of Rh/SiO$_2$ in glycerol reaction under hydrogen. *Green Chem.* **2007**, *9*, 582–588. [CrossRef]

21. Amada, Y.; Koso, S.; Nakagawa, Y.; Tomishige, K. Hydrogenolysis of 1,2-Propanediol for the Production of Biopropanols from Glycerol. *ChemSusChem* **2010**, *3*, 728–736. [CrossRef] [PubMed]

22. Ryneveld, E.V.; Mahomed, A.S.; Heerden, P.S.V.; Friedrich, H.B. Direct Hydrogenolysis of Highly Concentrated Glycerol Solutions over Supported Ru, Pd and Pt Catalyst Systems. *Catal. Lett.* **2011**, *141*, 958–967. [CrossRef]

23. Li, C.; He, B.; Ling, Y.; Tsang, C.W.; Lian, C. Glycerol hydrogenolysis to n-propanol over Zr-Al composite oxide-supported Pt catalysts. *Chin. J. Catal.* **2011**, *39*, 1121–1128. [CrossRef]

24. Wang, M.; Yang, H.; Xie, Y.; Wu, X.; Chen, C.; Ma, W.; Dong, Q.; Hou, Z. Catalytic transformation of glycerol to 1-propanol by combining zirconium phosphate and supported Ru catalysts. *RSC Adv.* **2016**, *6*, 29769. [CrossRef]

25. Schlaf, M.; Ghosh, P.; Fagan, P.J.; Hauptman, E.; Bullock, R.M. Catalytic Deoxygenation of 1,2-Propanediol to Give n-Propanol. *Adv. Synth. Catal.* **2009**, *351*, 789–800. [CrossRef]

26. Zhu, S.; Zhu, Y.; Hao, S.; Zheng, H.; Mo, T.; Li, Y. One-step hydrogenolysis of glycerol to biopropanols over Pt–$H_4SiW_{12}O_{40}$/ZrO_2 catalysts. *Green Chem.* **2012**, *14*, 2607–2616. [CrossRef]

27. Priya, S.S.; Kumar, V.P.; Kantam, M.L.; Bhargava, S.K.; Periasamy, S.; Chary, K.V.R. Metal–acid bifunctional catalysts for selective hydrogenolysis of glycerol under atmospheric pressure: A highly selective route toproduce propanols. *Appl. Catal. A Gen.* **2015**, *498*, 88–98. [CrossRef]

28. Lin, X.; Lv, Y.; Xi, Y.; Qu, Y.; Phillips, D.L.; Liu, C. Hydrogenolysis of Glycerol by the Combined Use of Zeolite and Ni/Al_2O_3 as Catalysts: A Route for Achieving High Selectivity to 1-Propanol. *Energy Fuels* **2014**, *28*, 3345–3351. [CrossRef]

29. Zhang, Y.; Han, W.; Long, X.; Nie, H. Redispersion effects of citric acid on CoMo/-Al_2O_3 hydrodesulfurization catalysts. *Catal. Commun.* **2016**, *82*, 20–23. [CrossRef]

30. Meng, D.; Wang, B.; Yu, W.; Wang, W.; Li, Z.; Ma, X. Effect of Citric Acid on MoO_3/Al_2O_3 Catalysts for Sulfur-Resistant Methanation. *Catalysts* **2017**, *7*, 151. [CrossRef]

31. Halasz, I.; Brenner, A. Preparation and characterization of PdO-MoO & Al_2O_3 catalysts. *Appl. Catal. A Gen.* **1992**, *82*, 51–63.

32. Del Arco, M.; Carrazan, S.R.G.; Martin, C.; Martin, I.; Rives, V.; Maletb, P. Surface dispersion of molybdena supported on silica, alumina and titania. *J. Mater. Chem.* **1993**, *3*, 1313–1318. [CrossRef]

33. Yang, X.L.; Dai, W.L.; Gao, R.; Fan, K. Characterization and catalytic behavior of highly active tungsten-doped SBA-15 catalyst in the synthesis of glutaraldehyde using an anhydrous approach. *J. Catal.* **2007**, *249*, 278–288. [CrossRef]

34. Barras, J.; Klinowski, J. 27AI and 29Si Solid-state NMR Studies of Dealuminated Mordenite. *J. Chem. Soc. Faraday Trans.* **1994**, *90*, 3719–3723. [CrossRef]

35. Priya, S.S.; Bhanuchander, P.; Kumar, V.P.; Deepa, D.; Selvakannan, P.R.; Kantam, M.L.; Bhargava, S.K.; Chary, K.V.R. Platinum supported on H-Mordenite: A highly efficient catalyst for selective hydrogenolysis of glycerol to 1,3-PDO. *ACS Sustain. Chem. Eng.* **2016**, *4*, 1212–1222. [CrossRef]

36. Oh, J.; Dash, S.; Lee, H. Selective conversion of glycerol to 1,3-propanediol using Pt-sulfated Zirconia. *Green Chem.* **2011**, *13*, 2004–2007. [CrossRef]

37. Priya, S.S.; Kumar, V.P.; Kantam, M.L.; Bhargava, S.K.; Srikanth, A.; Chary, K.V.R. High Efficiency Conversion of Glycerol to 1,3-Propanediol Using a Novel Platinum−Tungsten Catalyst Supported on SBA-15. *Ind. Eng. Chem. Res.* **2015**, *54*, 9104–9115. [CrossRef]

38. Priya, S.S.; Bhanuchander, P.; Kumar, V.P.; Bhargava, S.K.; Chary, K.V.R. Activity & Selectivity of Platinum-Copper bimetallic catalysts supported on mordenite for glycerol hydrogenolysis to 1,3-propanediol. *Ind. Eng. Chem. Res.* **2016**, *55*, 4461–4472.

39. Priya, S.S.; Kumar, V.P.; Kantam, M.L.; Bhargava, S.K.; Chary, K.V.R. Vapour-Phase Hydrogenolysis of Glycerol to 1,3-Propanediol Over Supported Pt Catalysts: The Effect of Supports on the Catalytic Functionalities. *Catal. Lett.* **2014**, *144*, 2129–2143. [CrossRef]

40. Amada, Y.; Shinmi, Y.; Koso, S.; Kubota, T.; Nakagawa, Y.; Tomishige, K. Reaction mechanism of the glycerol hydrogenolysis to 1,3-propanediol over Ir-ReOx/SiO_2 catalyst. *Appl. Catal. B Environ.* **2011**, *105*, 117–127. [CrossRef]

41. Huang, L.; Zhu, Y.; Zheng, H.; Ding, G.; Li, Y. Direct conversion of glycerol into 1,3-propanediol over Cu-$H_4SiW_{12}O_{40}$/SiO_2 in vapor phase. *Catal. Lett.* **2009**, *131*, 312–320. [CrossRef]

42. Cavani, F.; Guidetti, S.; Trevisanut, C.; Ghedini, E.; Signoretto, M. Unexpected events in sulfated zirconia catalyst during glycerol-to-acrolein conversion. *Appl. Catal. A Gen.* **2011**, *409–410*, 267–278. [CrossRef]

43. Miyazawa, T.; Kusunoki, Y.; Kunimori, K.; Tomishige, K. Glycerol conversion in the aqueous solution under hydrogen over Ru/C + an ion-exchange resin and its reaction mechanism. *J. Catal.* **2006**, *240*, 213–221. [CrossRef]

44. Kumar, V.P.; Priya, S.S.; Harikrishna, Y.; Kumar, A.; Chary, K.V.R. Catalytic Functionalities of Nano Ruthenium/γ-Al_2O_3 Catalysts for the Vapour Phase Hydrogenolysis of Glycerol. *J. Nanosci. Nanotechnol.* **2016**, *16*, 1952–1960. [CrossRef]

45. El-Shobakya, H.G.; Mokhtarb, M.; Ahmeda, A.S. Effect of MgO-doping on solid-solid interactions in MoO$_3$/Al$_2$O$_3$ system. *Thermochim. Acta* **1999**, *327*, 39–46. [CrossRef]

46. Toniolo, F.S.; Barbosa-Coutinho, E.; Schwaab, M.; Leocadio, I.C.L.; Aderne, R.S.; Schmal, M.; Pinto, J.C. Kinetics of the catalytic combustion of diesel soot with MoO$_3$/Al$_2$O$_3$ catalyst from thermogravimetric analyses. *Appl. Catal. A Gen.* **2008**, *342*, 87–92.